

# Laser Amplifier Development for IPDA Lidar measurements of CO<sub>2</sub> from Space

Anthony W. Yu <sup>\*a</sup>, James B. Abshire <sup>a</sup>, Mark Storm <sup>b</sup>, Alexander Betin <sup>c</sup>

<sup>a</sup> NASA Goddard Space Flight Center, Greenbelt MD USA 20771;

<sup>b</sup> Fibertek, Herndon VA 20171;

<sup>c</sup> Raytheon Space and Airborne Systems, El Segundo, CA, USA 90245

## ABSTRACT

Accurate global measurements of tropospheric CO<sub>2</sub> mixing ratios are needed to better understand the global carbon cycle and the CO<sub>2</sub> exchange between land, oceans and atmosphere. NASA Goddard Space Flight Center (GSFC) is developing a pulsed lidar approach for an integrated path differential absorption (IPDA) lidar as a candidate for the NASA's planned ASCENDS mission to allow global measurements of atmospheric CO<sub>2</sub> column densities from space. Our group has developed and demonstrated an airborne IPDA lidar for this purpose. It uses two tunable pulsed laser transmitters allowing simultaneous measurement of a single CO<sub>2</sub> absorption line in the 1570 nm band, absorption of an O<sub>2</sub> line pair in the oxygen A-band (765 nm), and atmospheric backscatter profiles in the same path. In the airborne lidar, both lasers are pulsed at 10 kHz, and the two absorption line regions are sampled at typically a 300 Hz rate.

A space version of this lidar must have a much larger laser power-telescope area product to compensate for the signal losses in the ~40x longer range. An analysis of signal to noise ratios indicated that for a 400 km orbit, a 1.5 m diameter telescope and a 10 second integration time, that 1.5 to 2 mJ laser energy is required to attain the needed measurement precision. To meet the laser energy requirements we have pursued two parallel power-scaling approaches for the space laser. These include a single-amplifier approach consists of a multi-pass Er:Yb:Phosphate glass based planar waveguide amplifier (PWA) and a parallel amplifier approach using multiple (typically 8) large mode area (LMA) fiber amplifiers. In this paper we summarize the laser amplifier design approaches and preliminary results.

**Keywords:** CO<sub>2</sub> lidar, laser spectroscopy, solid-state laser amplifier, space laser transmitter, fiber amplifier

## 1. INTRODUCTION

We are conducting research on a laser sounder instrument for global measurements of atmospheric CO<sub>2</sub> in support of the future Active Sensing of CO<sub>2</sub> Emissions over Nights, Days, and Seasons (ASCENDS) mission.<sup>1</sup> Although increasing atmospheric CO<sub>2</sub> is widely accepted as the largest anthropogenic factor causing climate change, there is considerable uncertainty about its global budget. Accurate measurements of tropospheric CO<sub>2</sub> mixing ratios are needed to study CO<sub>2</sub> emissions and CO<sub>2</sub> exchange with the land and oceans. To be useful in reducing uncertainties about carbon sources and sinks the atmospheric CO<sub>2</sub> measurements need spatial resolution at the several degree level and ~ 0.3% precision.

Our group has developed a pulsed lidar approach as a candidate for the ASCENDS mission (Figure 1).<sup>2,3</sup> Our approach uses an erbium doped fiber amplifier (EDFA) based laser for atmospheric CO<sub>2</sub> measurements in an overtone band near 1572 nm.<sup>4</sup> It uses a dual band pulsed laser absorption spectrometer and the integrated path differential absorption (IPDA) for the laser sounder technique.<sup>5</sup> The approach uses two tunable pulsed laser transmitters allowing simultaneous measurement of the absorption from a CO<sub>2</sub> absorption line in the 1570 nm band, O<sub>2</sub> absorption in the oxygen A-band (765 nm), range (scattering surface elevation) and atmospheric backscatter profiles in the same path.

The lidar operates by stepping a tunable laser in wavelength across a single CO<sub>2</sub> line for the CO<sub>2</sub> column measurement, while simultaneously another laser is stepped across an O<sub>2</sub> line pair near 765 nm in the Oxygen A-band for an atmospheric pressure measurement.<sup>6,7</sup> For space the present plan is to pulse both lasers at a ~8 kHz rate, resulting in both absorption line regions being sampled in wavelength every ~ 1 msec. The direct detection receiver measures the time resolved laser backscatter at both wavelengths from the atmosphere along with the energies of the laser echoes from the surface. After suitable averaging the gas extinction and column densities for the CO<sub>2</sub> and O<sub>2</sub> gases are calculated from the sampled wavelengths of the surface reflected line shapes via the IPDA lidar technique.<sup>8</sup>

We selected a flexible MOPA architecture for the laser transmitters. This allows narrow-linewidth frequency-tunable seed lasers to be used to meet the wavelength stability and tunability requirement for sampling the CO<sub>2</sub> and O<sub>2</sub> gas absorption features, and using subsequent amplifier stages to attain the needed energy. We have recently demonstrated a wavelength-locked laser source that rapidly steps through eight or more wavelengths distributed across a 1572.335 nm CO<sub>2</sub> absorption line to allow precise measurements of atmospheric CO<sub>2</sub> absorption. A similar approach can be used for the 1529 nm wavelength band and then frequency doubled to generate the 764.7 nm for the O<sub>2</sub> measurements.

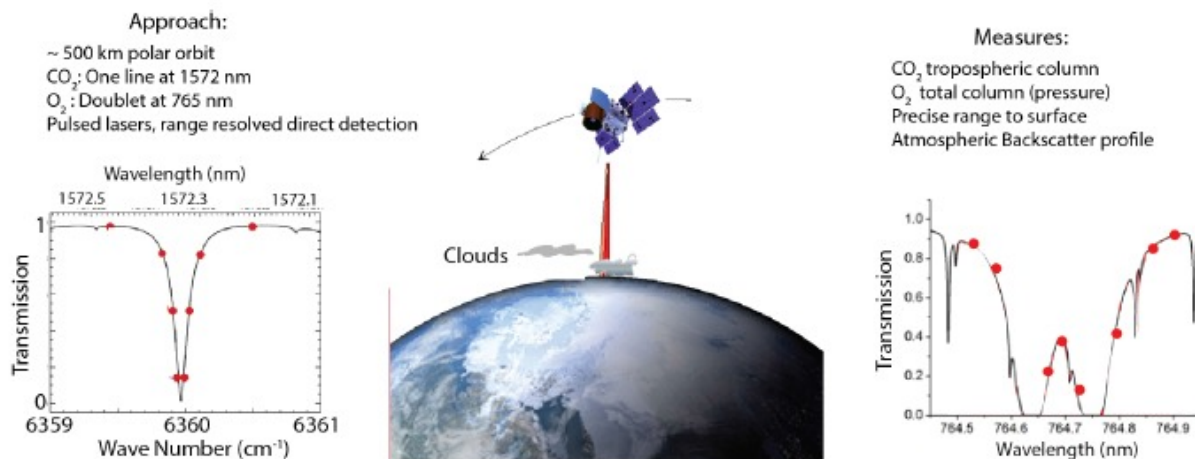


Figure 1. The GSFC CO<sub>2</sub> Laser Sounder approach, which measures the column CO<sub>2</sub> & O<sub>2</sub> absorption and range to the scattering surface from space. (Left) Nominal CO<sub>2</sub> line (1572.33 nm) targeted for use for 2-way pass to surface from space. The laser sounder measures the shape and depth of this CO<sub>2</sub> line and the absorption of a line doublet near 764.7 nm in the O<sub>2</sub> A-band (Right). The line sampling approach is flexible and for space the present plan is 8-wavelength samples/line.

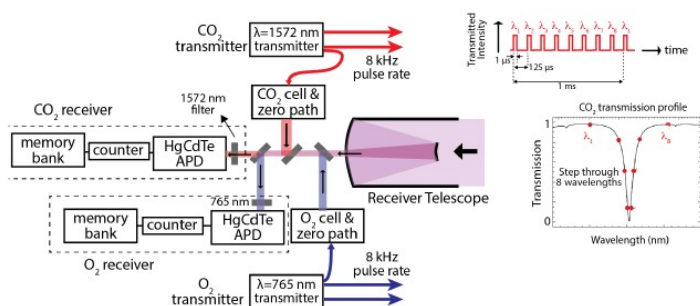


Figure 2. Block diagram of the space lidar instrument. Simultaneous measurements are made of CO<sub>2</sub>, and O<sub>2</sub>, absorption line shapes, time of flight, and backscatter profiles at 1572.33 nm and 764.7 nm wavelengths. The backscattered signal is collected by a common 1.5-m telescope and detected.

Table 1. A summary of the present version of laser requirements for space. The requirements were based on feedback from airborne campaigns and from an analytical model of the space-based lidar measurement and receiver.

Performance Parameter	Laser Transmitter Overall Performance
Center Wavelength	1572.335 nm and 1529 nm
Tuning speed	NA
Linewidth	≤ 100 MHz
Side-mode suppression ratio (spectral)	>30 dB
Pulse repetition frequency	7.5 KHz
Pulse period (derived)	133 μs
Pulse Width	100 ns – 1 μs (assume 1 μs)
Duty Cycle (derived)	0.75 %
Pulse shape	Trapezoidal
Pulse energy	>3.2 mJ (goal); >2.5 mJ (operating)
Average power (informational derived)	>24 W (goal); 20 W (operating)
Peak power	3.2 KW goal; 2.5 kW operating
PER [TBR]	20 dB
Wall-plug Efficiency	> 10% (goal)

Since 2008 our group has participated in several ASCENDS airborne campaigns. These have allowed demonstrating the measurement concepts and measurements over a wide variety of surface and atmospheric conditions.<sup>9,10,11</sup> To scale for space, the energy per pulse in each of these wavelengths (1529 nm and 1572 nm) needs to be increased to appropriate levels. A space-based version of this lidar must have a much larger lidar power-area product due to the ~x40 longer range (see Figure 2). We have developed models to estimate the measurement SNR for both the CO<sub>2</sub> and O<sub>2</sub> channels and applied them to estimate lidar parameters needed for the space measurement (see Table 1). Our initial calculations

show for a 400 km orbit, a 1.5 m diameter telescope and a 10 second integration time, which allows a 70 km along track integration in low earth orbit, that 1.5 to 2 mJ laser pulse energy is required to attain the measurement precision.

For mission like ASCENDS, the need is measure the column average CO<sub>2</sub> mixing ratio, which required an additional estimate of the dry air column density. The mixing ratio is insensitive to fluctuations in surface pressure resulting from changing topography or weather systems and to fluctuations in temperature and humidity. For the O<sub>2</sub>, column measurements, we have chosen an approach using a 1529 nm DFB-laser-diode oscillator frequency-doubled erbium-fiber-amplifier (1529nm/764.5nm) MOPA transmitter.<sup>12</sup> More recently we have achieved over 1 kW peak power from a 1529 nm fiber amplifier.<sup>13</sup>

## 2. LASER TRANSMITTER

### 2.1 Laser Architecture

The space-based lidar uses a master oscillator power amplifier (MOPA) approach for the laser. The MOPA laser consists of a tunable narrow linewidth diode master oscillator seed a laser follows by two multi-stage power amplifiers. This modular approach is flexible and has a number of advantages. A key one is that it leverages the lower power seed laser and amplifier stages we have already demonstrated and scales it to space by adding power amplifiers. The diode seed lasers for the CO<sub>2</sub> and O<sub>2</sub> wavelengths are highly developed, and have been space qualified. To meet the precision, the online lasers need to be frequency stabilized to ~1 MHz.<sup>14</sup> We have frequency locked the master laser diode to the CO<sub>2</sub> line center and achieved frequency drifts < 0.3 MHz over 72 hours. We have demonstrated a new step-locked single laser diode source that accurately locks its output to 8 or more wavelengths around the CO<sub>2</sub> absorption line. This allows a significant simplification to the seed laser stage.

### 2.2 Master Oscillator

The master oscillator (MO) is based on a distributed-feedback laser diode (DFB-LD). In laboratory tests this laser has been frequency-locked to the CO<sub>2</sub> line center by using a frequency modulation technique, limiting its peak-to-peak frequency drift to 0.3MHz at 0.8 s averaging time over 72 hours.<sup>15</sup> Four online DFB-LDs were then offset locked to this laser using phase-locked loops, retaining virtually the same absolute frequency stability.<sup>16</sup> These online and two offline DFB-LDs were subsequently amplitude switched and combined. This produced a precise wavelength stepped laser pulse train, to be amplified for CO<sub>2</sub> measurements.<sup>17</sup> Figure 3 shows the concept for a master oscillator approach that produces a programmable number of wavelength steps using a step-locked approach.

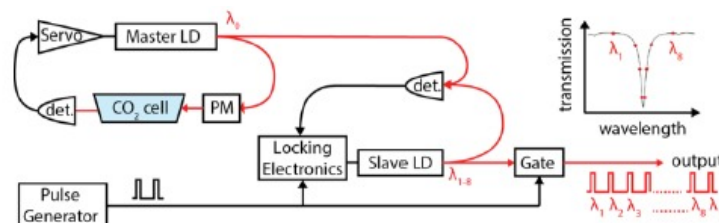


Figure 3. Schematic of a stepped wavelength locked source. The master wavelength is locked to a CO<sub>2</sub> absorption cell. By offset-locking a slave laser at different frequency offsets to the master, a pulse train step-locked 8 discrete points on 1572.335 nm CO<sub>2</sub> line was generated.

### 2.3 Power Amplifier Approaches

#### 2.3.1 Single Power Amplifier Approach – Er:Yb:Phosphate Planar Waveguide Amplifier

We are pursuing a single power amplifier (PA) approach led by Raytheon Space and Airborne Systems (RSAS) to meet the energy requirement for the CO<sub>2</sub> and O<sub>2</sub> sensing from space. The seed laser input for this approach is the laser transmitter from our airborne lidar that uses a commercial EDFA as a preamplifier. In the airborne transmitter, it emits a 1 μsec wide pulses at a 10 kHz rate with 25 W peak power, with a pulse energy of 25 μJ and 250 mW average power. The approach for the amplifier for both wavelengths is schematically shown in Figure 4, which uses a custom Er:Yb:Phosphate planar waveguide amplifier (PWA) preceded by a fiber pre-amplifier. In our previous effort with

RSAS, they have successfully produced and demonstrated the advantages of PWA for swath mapping application.<sup>18</sup> The power scaling for CO<sub>2</sub> and O<sub>2</sub> sensing at the 1572 and 1529 nm bands requires careful selection of material and efficient amplifier design since these wavelength are on either end of the gain spectrum of typical erbium glass. For space use, appropriate pump and gain confinement are needed in a reasonably sized package. The erbium-doped phosphate glass was chosen because it provides a broad gain spectrum, and Er:Yb co-doping allows the use of space qualified 940nm pump diode modules.<sup>19</sup> The planar waveguide (PWG) concept, which is based on Raytheon's proprietary technology, was chosen for its advantages of efficient gain confinement and thermal management.<sup>20</sup>

The first approach considered for the amplifier was based on double passing the input signal from the MO and preamplifier in the PWG as shown in Figure 4. The output energies and efficiencies calculated from RSAS's laser amplifier model are summarized in Table 2. Figure 5 illustrates the generic PWG design. The PWG is essentially a flat fiber in which the core is index-guided in the narrow dimension and is unguided in the wide dimension. The signal is mode matched into the core that has a typical dimension of ~10 to 200µm. The high aspect ratio of the PWG design provides a large surface area for efficient cooling. In our approach, the PWG will be cladding pumped by power combining three 940 nm pump laser diode arrays.

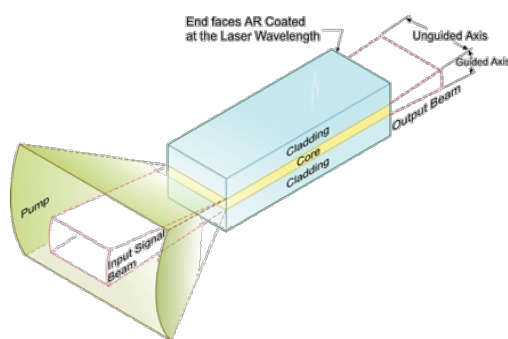
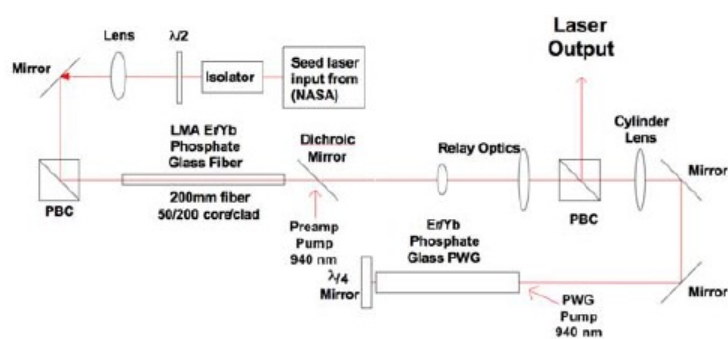


Figure 4. Schematic of the MOPA laser transmitter consists of multi-pass planar waveguide amplifier approach for power scaling.

Figure 5. Typical planar waveguide structure.

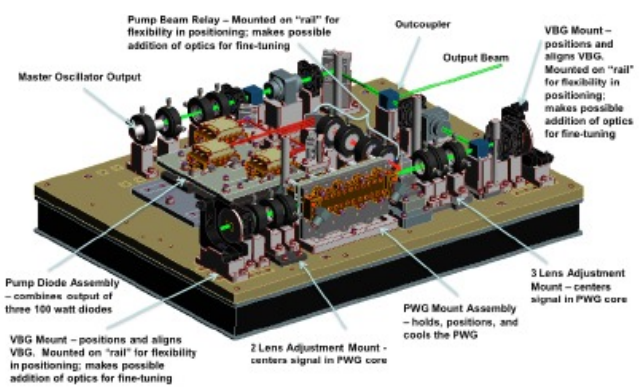
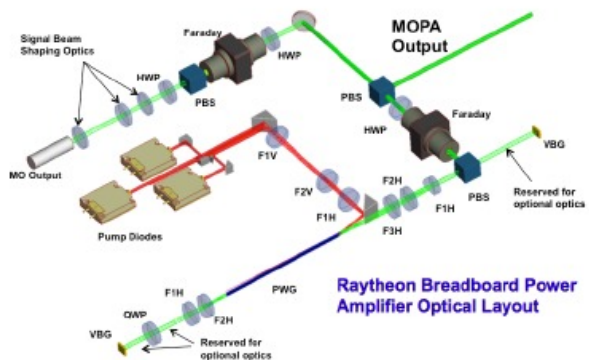


Figure 6. (Left) Optical beam path of the multi-pass PWA that is being assembled. The PWG is pumped by three 940 nm laser diodes. Narrow band mirrors using volume Bragg gratings (VBGs) are used to reject out of band ASE and gain. (Right) CAD of the breadboard PA for the optical layout on the left. The overall dimension is ~24" x 18" x 6".

In the present program RSAS is completing the development of a four-pass PWG-based power amplifier breadboard shown in Figure 6. The attractiveness of four-pass approach is in eliminating the need for a pre-amplifier. In addition, the requirement for single pass amplifier gain is reduced by the use of volume Bragg gratings (VBGs) as reflectors to suppress the ASE and parasitic oscillations at unwanted peak gain wavelength (~1555 nm). The PWG is ~150mm long Er:Yb:Phosphate with overall cross section dimension of 0.5 mm (tall) x 5 mm (wide). Four-pass amplifier model predicts >4 mJ output pulse at ~300W of diode pump power with 20 µJ of input pulse energy from a seed laser. The

wall-plug efficiency has been calculated to be ~8%. RSAS is in the process of assembling a breadboard of this Er:Yb:Glass PWG-based laser amplifier and evaluating its capabilities. Several PWG designs have already been fabricated and delivered for early evaluation.

Table 2. Modeling results of PWG performance at different wavelengths for CO<sub>2</sub> and O<sub>2</sub> sensing.

Wavelength	PWG Pump Power @ 3 mJ Output Energy	Efficiency @ 3 mJ Output Energy	Max PWG Pump Power	PWG Output Energy @ Max Pump	Efficiency @ Max Pump Power
1569 nm	170 W	8.4%	400 W	8.7 mJ	10.3%
1572 nm	190 W	7.5%	400 W	6.7 mJ	8.0%
1575 nm	240 W	6.0%	400 W	4.2 mJ	5.0%
1529.6 nm	160 W	9.0%	400 W	7.3 mJ	8.7%

The fabrication and manufacturing processes for PWG's in crystalline-based gain materials is mature and several of these waveguides have been successfully delivered and demonstrated. However, the manufacturing process for glass based PWGs is still being refined. Several Er:Yb:Phosphate glass PWGs have been fabricated that have the correct core thickness but varying cladding thicknesses have been assembled and being evaluated at RSAS (see Figure 7).

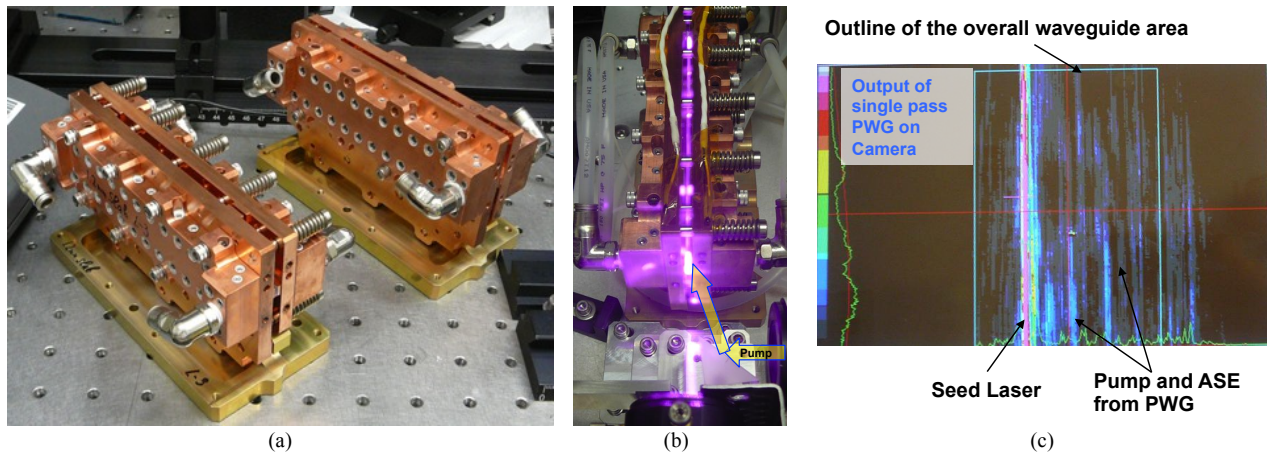


Figure 7. (a) Assembled PWGs, sandwiched between two water-cooled heat sinks and spring loaded mechanical mount for efficient thermal management; (b) One of the assembled PWG modules is being pumped by 940 nm pump diodes; (c) A beam profiling camera capturing the seed laser, unabsorbed pump light and amplified spontaneous emission from the PWG module shown in (b). The green line outlines the dimension of the overall PWG.

The initial evaluation has confirmed that the cladding thicknesses played a significant role in pump confinement, which leads to how efficient pump light will be absorbed by the gain medium and leakage of unabsorbed pump out of the PWG. Nevertheless, preliminary tests of the amplifier performance, with the available PWG slab installed, resulted in demonstration of more than unity net gain for single, two and four-pass arrangements. The new PWGs fabricated to meet our designed dimensions are close to completion. We will report the performance of this power amplifier in the near future.

### 2.3.2 Multiple Amplifier Approach – Parallel Large Mode Area Fiber Amplifiers

We are also pursuing a parallel path using an all-fiber laser approach to meet the ASCENDS requirements. The laser design is based on an advanced, eye-safe, polarization-maintaining (PM) MOPA lidar transmitter platform that was under development at Fibertek.<sup>21,22,23,24,25,26</sup> This platform consists of a narrow linewidth (400 Hz - 1MHz) seed laser, a flexible and reconfigurable pulse generator, and multiple stages of PM EDFA with increasing mode-field area. Using this approach, we have demonstrated up to 475 μJ energy per pulse at 1572.3 nm, and up to 250 μJ energy per pulse at 1529 nm wavelength with 1.5 μs pulse widths at 10 kHz pulse rates. The output beams at the highest energy levels were diffraction limited, and the polarization extinction ratio (PER) was ~17dB. The optical to optical conversion efficiency was ~17% with respect to total pump power.

### 2.3.2.1 CO<sub>2</sub> Channel – Power Scaling of 1572 nm

To attain ~2 mJ per pulse energy, the plan is to use multiple (typically 8) fiber amplifiers in parallel. The output beams are overlapped (incoherently combined) in the far field to provide the required energy for the lidar measurement. The power amplifier chains utilize the same seed laser to ensure the system operates at a single wavelength. A prototype fiber amplifier breadboard based on an all-fiber MOPA architecture based on Fibertek heritage systems utilizing PM fiber components and operated in single transverse mode. The obtained energy levels at 1572.3 nm at each stage are illustrated in Figure 8.

The MO is a 15 mW DFB laser diode with a center wavelength of ~1572.3 nm. The MO was operated in continuous-wave (CW) mode for best wavelength stability and narrowest linewidth of <1 MHz.

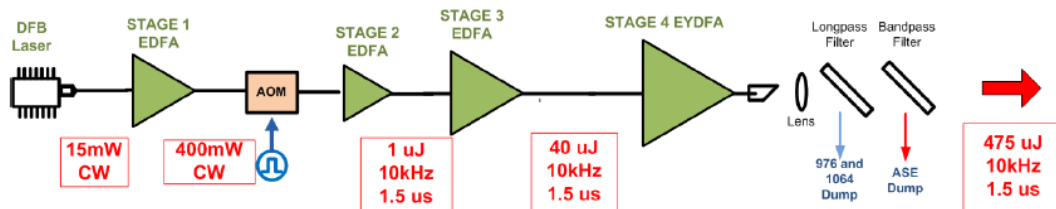


Figure 8. Experimental setup with illustrated 1572.3 nm power/energy levels at each stage.

The first stage is a CW EDFA amplifier that provides a high signal level into the pulse shaping acousto-optic modulator (AOM) in order to provide the highest energy to the subsequent amplifier stages. At the 1570nm band, the gain of the EDFA is lower, so using amplifier saturation is extremely important to achieve the lowest amplified spontaneous emission (ASE) noise. The stage 1 EDFA is built with Er/Yb co-doped PM single-mode fiber and pumped with a broad area 976 nm laser diode. The amplifier has an 18 nm band pass filter, centered at 1570 nm at the output. This amplifier can operate up to ~400 mW.

Pulse shaping at 10 kHz from the amplified CW signal is achieved by using a high extinction ratio (~47 dB) AOM. The overall intrinsic loss of the modulator is ~3dB. The AOM was driven by arbitrarily shaped pulse waveforms in order to reduce the effects of pulse steepening in the fiber amplifier chain. In this effort, the leading edge of the pulse is pre-attenuated in order to compensate for the higher gain experienced by this edge. Figure 9 shows the optical spectrum of the amplified output and a sample waveform demonstrating this mentioned pre-distortion of the pulse, and how this pulse corrects through the power amplifier.

The second stage EDFA is built with a highly doped, single mode PM erbium doped fiber and pumped with a telecom grade single mode frequency stabilized pump diode. This amplifier serves as a low energy preamplifier module for the stage 3 amplifier, and produces ~ 1  $\mu$ J energy at 10 kHz. The stage 3 EDFA is built with the same fiber that is used in stage 1 EDFA, and generates up to 40  $\mu$ J energy at 10 kHz.

The final power amplifier stage, EDFA 4, employed a commercial PM large mode area (LMA) fiber with 25  $\mu$ m core diameter. The amplifier was counter-pumped by a tandem of 975 nm pump lasers, with up to 50 W of pump power coupled into the gain fiber through a custom PM fused fiber combiner. A 1% tap monitor is used for forward and reverse Stimulated Brillouin Scattering (SBS) monitoring.

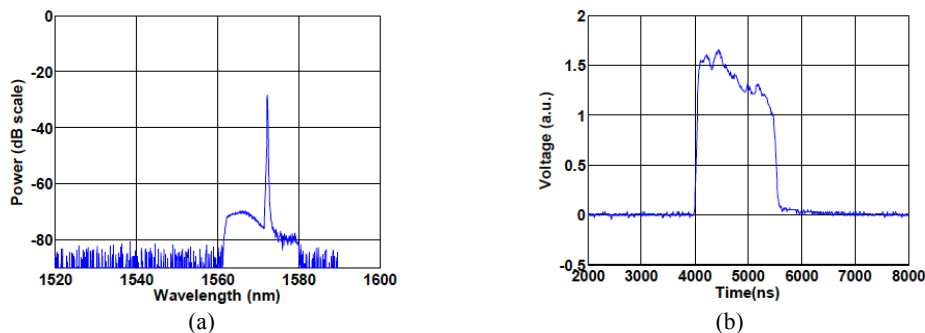


Figure 9. (a) Stage 1 EDFA output spectrum at 80 mW output (b), after power amplifier.

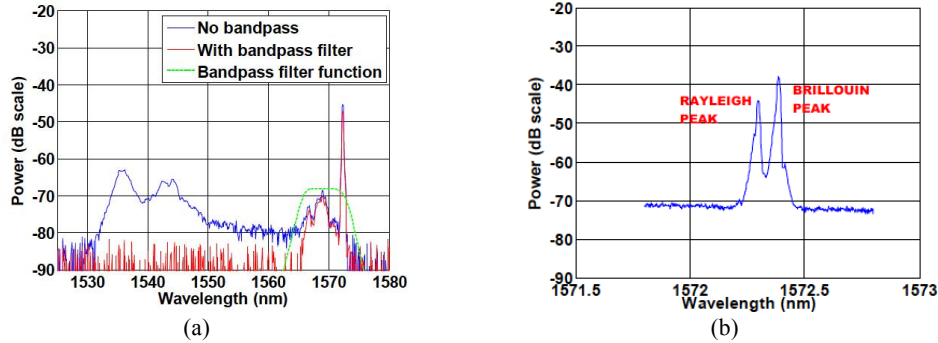


Figure 10. EDFA4 output at 1572.3 nm, 156  $\mu\text{J}$ , 10 kHz,  $\sim 1$  MHz linewidth,  $\sim 1.4$   $\mu\text{s}$  pulse width. (a) Output optical spectrum with and without band pass filter, (b) backward SBS spectrum.

With this amplifier, and the  $\sim 1$  MHz linewidth seed source, we obtained up to  $\sim 156$   $\mu\text{J}$  and is SBS-limited. We define the SBS threshold as when the backward scattered Brillouin spectral peak reaches the same relative intensity as the backward scattered Rayleigh spectral peak. When compared to the forward energy, this definition of SBS threshold is very conservative. In fact, our measurements show that, the absolute backscattered light (including Rayleigh and SBS light) is  $>40$  dB below the forward energy with this SBS threshold definition.

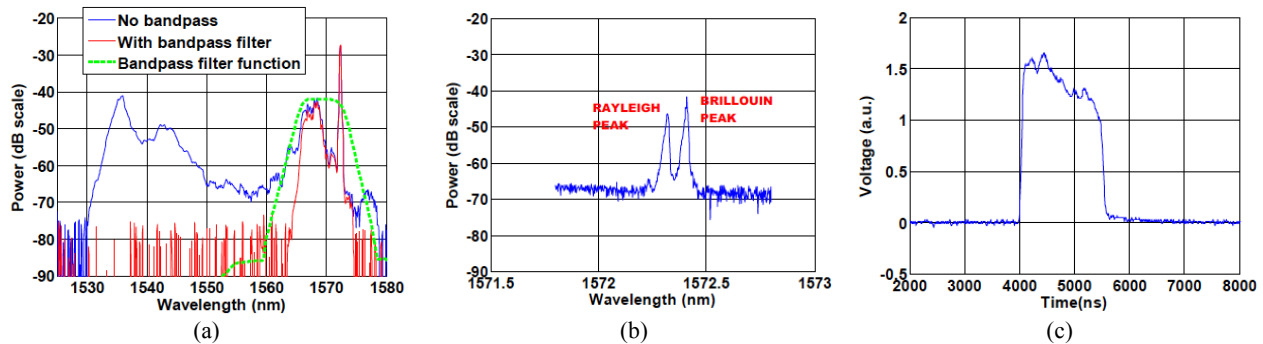


Figure 11. EDFA4 output at 1572.3 nm, 475  $\mu\text{J}$ , 10 kHz,  $\sim 100$  MHz seed laser linewidth,  $\sim 1.5$   $\mu\text{s}$  pulse width. (a) Output optical spectrum with and without band pass filter, (b) backward SBS spectrum, and (c) output pulse shape.

The output optical spectrum at 156  $\mu\text{J}$  (with and without band pass filter), backwards spectral plot, and output pulse shape plots are shown in Figure 10. The SBS peak is  $\sim 5$  dB above the Rayleigh peak, which is very slightly above SBS threshold.

Normally SBS is the main limiting factor for coherent (single frequency) fiber amplifiers, where the usual peak power threshold (limit) is on the order of 100-200 Watts for LMA fibers. The SBS free pulse energy could be further increased by broadening the seed laser linewidth. We were able to achieve up to 300  $\mu\text{J}$  energy at 50 MHz total bandwidth, and up to 475  $\mu\text{J}$  energy at 100 MHz total bandwidth for a 1.5  $\mu\text{s}$  pulse width as shown in Figure 11. The pump to signal optical to optical conversion efficiency was  $\sim 16.7\%$  with respect to the total pump power (not absorbed pump or slope).

The output beam quality (after the band pass filter) was measured at  $\sim 375$   $\mu\text{J}$  energy and was a single transverse mode with  $M^2$  estimated to be less than 1.2. The PER of the output was also measured at 375  $\mu\text{J}$  energy by rotating a high-extinction ratio polarizer and recording the maximum and minimum readings on the meter. The PER was  $\sim 17.26$  dB.

### 2.3.2.2 O<sub>2</sub> Channel – Power Scaling of 1529 nm

A laser wavelength at 765 nm is needed for O<sub>2</sub> sensing. Direct laser emission at this 765 nm wavelength is not readily available. Our approach is to generate a fundamental wavelength at 1529 nm and frequency doubled to 765 nm.<sup>6,7</sup> Here we describe our effort in power-scaling of the 1529 nm wavelength laser energy. The EDFA1 to EDFA3 for 1529 nm was re-optimized by shortening the gain fiber lengths, while the EDFA4 power amplifier stage used in the 1572 nm case remained unchanged in order to keep the gain fiber intact for future possible experiments. The obtained energy levels at 1529 nm at each stage are illustrated in Figure 12.

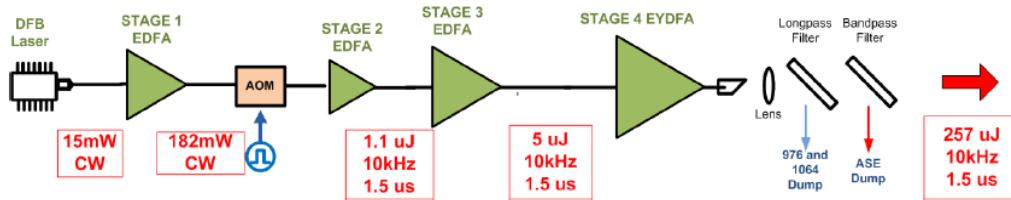


Figure 12. Experimental setup with illustrated 1529 nm power/energy levels at each stage

A DFB-LD with a center wavelength of  $\sim 1529$  nm and output power of up to 15 mW was used and, as previous case, was operated in CW mode for best wavelength stability and narrowest linewidth of  $<1$  MHz. The EDFA1 gain fiber was shortened from the 1572 nm case and we obtained up to 182 mW output average power at 1529 nm.

The second stage EDFA was kept the same as before, and produced  $\sim 1.1 \mu\text{J}$  energy at 10 kHz. The stage 3 EDFA gain fiber length was also reduced and we obtained  $\sim 5 \mu\text{J}$  from this stage, which limited the EDFA4 operation. Using the same EDFA4 configuration as in the earlier 1572 nm case, we obtained a pulse energy of  $\sim 161 \mu\text{J}$  with the 1529 nm seed operating at  $\sim 1$  MHz linewidth, which was also SBS-limited.

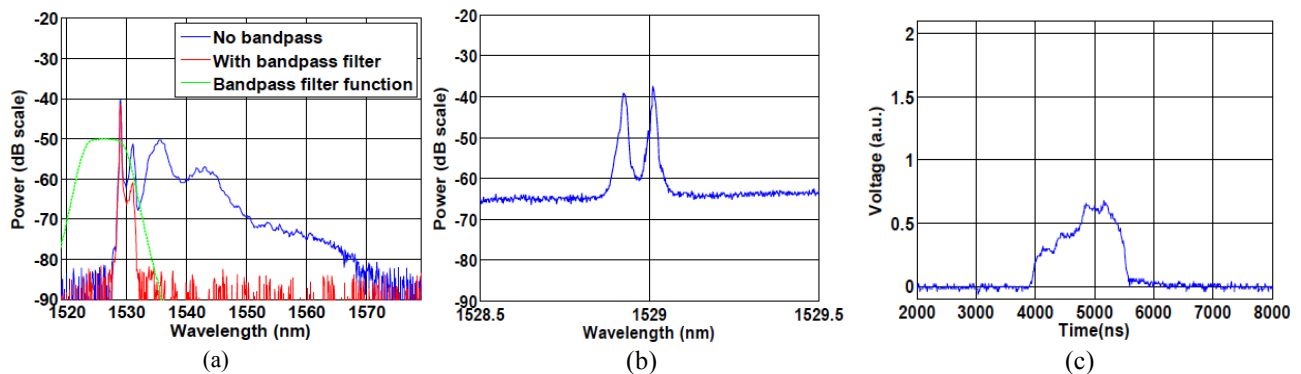


Figure 13. EDFA4 output at 1529 nm, 161  $\mu\text{J}$ , 10 kHz,  $\sim 1$  MHz seed laser linewidth,  $\sim 1.4 \mu\text{s}$  pulse width. (a) Output optical spectrum with and without band pass filter, (b) backward SBS spectrum, and (c) output pulse shape.

The output optical spectrum at 161  $\mu\text{J}$ , backwards spectral plot, and output pulse shape plots are shown in Figure 13. The FWHM is  $\sim 1.4 \mu\text{s}$  due to the non-square shape. With slight modifications to the pre-distorted pulse, the output pulse can be turned into a square shape.

With a 100 MHz DFB seed laser linewidth we achieved up to 257  $\mu\text{J}$  energy. The pulse was 1.5  $\mu\text{s}$  in width and square with mild structure that can be corrected with changes to the pre-distorted pulse that is fed into the AOM. The output beam quality was measured at the maximum 257  $\mu\text{J}$  energy and the beam was contained in a single transverse mode, with  $M^2$  estimated to be less than 1.2 in both directions. The PER of the output was also measured at 257  $\mu\text{J}$  energy by rotating a high-extinction ratio polarizer and recording the maximum and minimum readings on the meter. The PER was found to be  $\sim 17$  dB.

Table 3. Summary of the fiber amplifier breadboard results showing the achieved pulse energy at the 1572 and 1529 nm wavelengths and 1 MHz and 100 MHz spectral widths.

Wavelength [nm]	Repetition Rate [kHz]	Pulse Width [ $\mu\text{s}$ ]	Output Pulse Energy @ $<1$ MHz linewidth [ $\mu\text{J}$ ]	Output Pulse Energy @ 100 MHz linewidth [ $\mu\text{J}$ ]	Beam Quality, $M^2$	PER [dB]
1572.3	10	1.5	156	475	$<1.2$	17
1529	10	1.5	161	257	$<1.2$	17

In summary, we have successfully demonstrated power scaling of the  $\text{CO}_2$  and  $\text{O}_2$  channels at 1572 nm and 1529 nm wavelengths. Table 3 summarizes the achieved energy levels with corresponding spectral linewidths.



## CONCLUSIONS

We have made significant progress in developing the laser, and in power scaling laser energies for IPDA lidar measurements of CO<sub>2</sub> and O<sub>2</sub> column abundance from space. For the single amplifier approach using a PWA, preliminary results from thicker PWGs showed promising results. However, we are still awaiting the delivery of the PWG that meets our design parameters. For the parallel amplifier approach, we used fiber components from the telecommunication industry and successfully demonstrated results at 1572.3 nm and 1529 nm that are several times better than the published results in the literature. We are working on a follow-on effort to further develop the fiber amplifier approach with a direct path for space deployment.

## ACKNOWLEDGEMENT

The authors would like to acknowledge the support from NASA Earth Science Technology Office (ESTO) under the Advanced Component Technology (ACT), Innovative Incubator Program (IIP) and the Quick Response Study (QRS) awards, and NASA Goddard Space Flight Center Internal Research and Development (IRAD) program.

## REFERENCES

- [1]. NASA ASCENDS Mission Science Definition and Planning Workshop Report, Available from: [http://cce.nasa.gov/ascends/12-30-08%20ASCENDS\\_Workshop\\_Report%20clean.pdf](http://cce.nasa.gov/ascends/12-30-08%20ASCENDS_Workshop_Report%20clean.pdf), 2008.
- [2]. Abshire, J.B. et al., "A lidar approach to measure CO<sub>2</sub> concentrations from space for the ASCENDS Mission," Proc. SPIE 7832, paper 78320D, November 2010, doi:10.1117/12.868567.
- [3]. Kawa, S., et al., "Simulation studies for a space-based CO<sub>2</sub> lidar mission," Tellus B, 62, Dec. 2011.
- [4]. Abshire, J.B., et al. "Pulsed Airborne Lidar Measurements of Atmospheric CO<sub>2</sub> Column Absorption," Tellus Series B-Chemical And Physical Meteorology, 62 (5) pp. 770-783, 2010.
- [5]. Amediek, A., et al., "Analysis of Range Measurements From a Pulsed Airborne CO<sub>2</sub> Integrated Path Differential Absorption Lidar," IEEE Trans Geosci. Rem. Sensing, vol. PP, no. 99, pp.1-7, 2012, doi: 10.1109/TGRS.2012.2216884.
- [6]. Stephen, M.A., et al., "Narrowband, tunable, frequency-doubled, erbium-doped fiber-amplified transmitter," Optics Letters, Vol. 32, No. 15, pages 2073-6 (2007).
- [7]. Stephen, M.A., et al., "Oxygen Spectroscopy Laser Sounding Instrument for Remote Sensing of Atmospheric Pressure," IEEE Aerospace Conference, pages 1-6, doi: 10.1109/AERO.2008.4526388 (2008).
- [8]. Measures, R., Laser Remote Sensing: Fundamentals and Applications, Krieger Publishing, New York (1992).
- [9]. Abshire, J.B., et al., "Airborne measurements of CO<sub>2</sub> column absorption and range using a pulsed direct-detection integrated path differential absorption lidar," Appl. Opt. 52, 4446-4461 (2013).
- [10]. Abshire, J.B., et al., "Pulsed airborne lidar measurements of CO<sub>2</sub> column absorption," NASA ESTO ESTF-2011 Conference (2011), avail from: [http://esto.nasa.gov/conferences/estf2011/papers/Abshire\\_ESTF2011.pdf](http://esto.nasa.gov/conferences/estf2011/papers/Abshire_ESTF2011.pdf)
- [11]. Allan, G.R., et al., "Laser Sounder for Active Remote Sensing Measurements of CO<sub>2</sub> Concentrations", IEEE Aerospace Conference, doi: 10.1109/AERO.2008.4526387, Page(s): 1 – 7, 2008.
- [12]. Champert, P.A., et al., "Power scalability to 6 W of 770 nm source based on seeded fibre amplifier and PPKTP," Electronics Letters 37 (18): 1127-1129 Aug. 30 (2001).
- [13]. Wei, S., et al. "Kilowatt-level stimulated-Brillouin-scattering-threshold monolithic transform-limited 100 ns pulsed fiber laser at 1530 nm," Optics Letters 35(14) pp 2418-2420 (2010).
- [14]. Ehret, G., et al. "Space-borne remote sensing of CO<sub>2</sub>, CH<sub>4</sub>, and N<sub>2</sub>O by integrated path differential absorption lidar: A sensitivity analysis," Appl. Phys. B 90, 593–608, DOI: 10.1007/s00340-007-2892-3 (2008).
- [15]. Numata, K., et al., "Frequency stabilization of distributed-feedback laser diodes at 1572 nm for lidar measurements of atmospheric carbon dioxide," Appl. Opt., 50, 1047-1056 (2011).
- [16]. Numata, K., et al., "Precision and fast wavelength tuning of a dynamically phase-locked widely-tunable laser," Opt. Express, 20, 14234-14243 (2012).
- [17]. Numata, K., et al., "Frequency stabilization of distributed-feedback laser diodes at 1572 nm for lidar measurements of atmospheric carbon dioxide," Applied Optics, 50, 7, 1047, (2011).

- [18]. Yu, A.W. et al., "Highly Efficient Yb:YAG Master Oscillator Power Amplifier Laser Transmitter for Lidar Applications," in Conference on Lasers and Electro-Optics 2012, OSA Technical Digest (online), paper JTh11.6, 2012.
- [19]. Song, F. et al., "Spectra characteristics of novel Er:Yb phosphate glass," Proc. SPIE 3280, Rare-Earth-Doped Devices II, 46 (April 15, 1998); doi:10.1117/12.305406.
- [20]. Filgas, D., et al., "Recent Results for the Raytheon RELI Program," Laser Technology for Defense and Security VIII, edited by Mark Dubinskii, Stephen G. Post, Proc. of SPIE Vol. 8381 83810W, 2012. doi: 10.1117/12.921055.
- [21]. Akbulut M., et al., "Pulsed coherent fiber lidar transceiver for aircraft in-flight turbulence and wake-vortex hazard detection," Proc. SPIE 8037, Laser Radar Technology and Applications XVI, 80370R (7 June 2011); doi: 10.1117/12.883990.
- [22]. Akbulut, M., "Fiber Laser Coherent LIDAR for Wake-Vortex Hazard Detection," 16th Coherent Laser Radar Conference, 2011.
- [23]. Lu, W., "High-power, narrow linewidth 1.5- $\mu$ m fiber amplifier lidar transmitter for atmospheric CO<sub>2</sub> detection," Proc. SPIE 8961, Fiber Lasers XI: Technology, Systems, and Applications, 89610C (March 7, 2014); doi:10.1117/12.2041204
- [24]. Engin, D., et al., "Highly reliable and efficient 1.5 $\mu$ m-fiber-MOPA-based, high-power laser transmitter for space communication," Proc. SPIE 9081, Laser Technology for Defense and Security X, 90810G (9 June 2014); doi: 10.1117/12.2050496.
- [25]. Engin, D., et al., "Highly efficient and athermal 1550nm-fiber-MOPA-based high power down link laser transmitter for deep space communication," Proc. SPIE 8610, Free-Space Laser Communication and Atmospheric Propagation XXV, 86100G (19 March 2013), doi: 10.1117/12.2005926.
- [26]. Engin, D., et al., "Highly-efficient, high-energy pulse-burst Yb-doped fiber laser with transform limited linewidth," Proc. SPIE 9081, Laser Technology for Defense and Security X, 908112 (9 June 2014); doi: 10.1117/12.2050506.